Available online at www.sciencedirect.com
ScienceDirect
C. R. Mecanique 337 (2009) 517–527
COMPTES RENDUS MECANIQUE

Combustion for aerospace propulsion

The structure of multidimensional strained flames under transcritical conditions

L. Pons [a,*], N. Darabiha [a], S. Candel [a,b], T. Schmitt [c], B. Cuenot [c]

[a] *Laboratoire EM2C CNRS, École centrale Paris, 92295 Châtenay Malabry cedex, France*
[b] *Institut universitaire de France*
[c] *Cerfacs, 42, avenue G. Coriolis, 31100 Toulouse, France*

Available online 22 July 2009

Abstract

Strained flames are commonly used to study the structure of reactive layers and describe the local properties of turbulent combustion. This model is attractive because constant strain rate flames only depend on a transverse coordinate and can be treated as a one-dimensional problem. This configuration is considered in a multidimensional context in which the strained flow is obtained by two counterflowing streams of reactants. It is used to examine the structure of transcritical strained flames in which one or two reactants are injected at a high pressure exceeding the critical value while their temperature is below the critical value. Calculations are carried out in a two-dimensional domain to test numerical models developed for multidimensional simulations and test thermodynamic and transport models devised to deal with high pressure real gas effects. Multidimensional strained flame calculations carried out in this study serve to check the validity of a new version of a Navier–Stokes flow solver (AVBP) conceived to deal with transcritical combustion of interest to liquid propellant rocket applications. This article describes the basic elements of such simulations and discusses results of calculations. It is shown that the calculated multidimensional strained flames have the expected features in terms of structure and response to the imposed strain rate. ***To cite this article: L. Pons et al., C. R. Mecanique 337 (2009).***

Résumé

Structure des flammes étirées multidimensionnelles transcritiques. Les flammes étirées sont courrament utilisées pour analyser la structure de couches réactives et déterminer les propriétés locales d'une combustion turbulente. Ce modèle est pratique car la structure des flammes étirées ne dépend que de la coordonnée transverse et peut être traitée comme un problème unidimensionnel. Cette configuration est envisagée ici dans un contexte multidimensionnel dans lequel l'écoulement étiré est obtenu par deux jets réactifs à contre-courant. Elle est utilisée ici pour examiner la structure de flammes transcritiques dans lesquelles un au moins un des réactifs est injecté à une pression supérieure à la valeur critique mais à une température inférieure à la température critique. Les calculs réalisés dans un domaine bidimensionnel permettent de tester des méthodes numériques développés pour la simulation multi-dimensionnelle de la combustion transcritique. Ces calculs permettent de valider une nouvelle version d'un code de calcul Navier–Stokes (AVBP) adaptée au calcul d'écoulements réactifs transcritiques typiques des conditions de fonctionnement des moteurs-fusées à propulsion liquide. La méthodologie de calcul de tels écoulements est décrite et les résultats obtenus montrent que les flammes étirées transcritiques possèdent les propriétés attendues en termes de structure et de réponse à l'étirement. ***Pour citer cet article : L. Pons et al., C. R. Mecanique 337 (2009).***

* Corresponding author.
E-mail address: laetitia.pons@snecma.fr (L. Pons).

1631-0721/$ – see front matter
doi:10.1016/j.crme.2009.06.023

Keywords: Combustion; Transcritical combustion; Strained flame; High pressure

Mots-clés : Combustion ; Combustion transcritique ; Flamme étirée ; Haute pression

1. Introduction

Many practical systems like gas turbines, aero and automotive engines operate at elevated pressures. In liquid rocket engines (LRE), one of the reactants is injected in a liquid-like state, at a temperature which is below critical, in an environment where the pressure exceeds the critical value under conditions designated as "transcritical". In high performance cryogenic LREs the pressure takes values of the order of 10 MPa while the liquid oxygen stream is injected at 80 K. Combustion under such extreme conditions has been examined in recent experiments. The liquid oxygen/gaseous hydrogen flame structure is described in [1]. Jet flames formed by coaxial injection and combustion of transcritical oxygen with supercritical or transcritical methane are analyzed by Singla et al. [2]. One interesting finding is that coaxial injection of two transcritical reactants generates an unusual flame structure featuring two embedded conical regions of light emission indicating that combustion takes place in two separate layers of reaction. One reactive layer established in the vicinity of the oxygen jet boundary may be assimilated to a standard turbulent diffusion flame while the outer reactive layer forms near the dense methane boundary. The structure of flames formed by two transcritical propellants clearly differs from that observed in more standard conditions. Experiments on non-reacting transcritical injection carried out by Oschwald et al. [3] also indicate that the jet structure and mixing characteristics under subcritical and transcritical conditions are quite distinct. In the transcritical case, the dense low temperature transcritical fluid is bounded by a highly corrugated layer and mass is transferred from this region to the surrounding stream in a process which is governed by the local strain rates and heat fluxes.

The problem of transcritical combustion is also envisaged in recent numerical simulations. Calculations have to suitably describe real gas effects which characterize trans- and supercritical fluids. Improved equations of state for such conditions are proposed by Harstad et al. [4]. Simulations of mixing layers at high pressure are reported in [5,6] and more recently in [7], but the reactant streams are in a supercritical state. Their temperature exceeds the critical value which is less difficult to handle numerically than the transcritical fluids. The application of Large Eddy Simulations (LES) is explored in Ref. [8] in the case of a coaxial jet flame formed by injecting a transcritical oxygen stream. Calculations focus on the near vicinity of the coaxial injector in the case of transcritical oxygen/supercritical methane combustion. The flame is anchored in the wake region behind the LOx post and spreads in the near vicinity of the LOx jet boundary. Many other studies consider spherical droplets of transcritical fluids placed in a supercritical environment (see, for example, [9–11]). In the spherical geometry the problem is one-dimensional, greatly simplifying the analysis. However, experiments indicate that the process of atomization which governs subcritical liquid injection and gives rise to a droplet sprays is not operative in the transcritical range. There are no droplets but a highly wrinkled frontier separating the dense transcritical propellant from the surrounding lighter fluid. Mass transfer takes place from this dense jet and is essentially governed by the amount of exchange surface area and by the local turbulent state of the flow. This in turn depends on the local strain rate or scalar dissipation. Under such conditions it is natural to represent the local flame elements in terms of strained flames. The turbulent flame is then modeled as a collection of strained reactive layers which are convected and distorted by the flow but can be identified. The strained flame geometry envisaged in the present article is directly useful to the analysis of transcritical flames. A recent article [12] deals with the structure of transcritical oxygen/supercritical or transcritical methane counterflow flames and proposes a correlation for the mass transfer rate from the dense zone to the light region. The present article complements this effort in various directions. The main objectives are: (1) To develop a methodology for multidimensional counterflow flames; and (2) To validate a new version of the AVBP flow solver including real gas effects by examining the mass transfer rate and flame structure under transcritical conditions. This article begins with a brief description of the new version of AVBP and specifically considers thermodynamics and transport models included to account for real gas effects and transport anomalies. The methodology adopted for multidimensional strained flame calculations is described in Section 3.1. Results of simulations of counterflow configurations under high pressure conditions are discussed in Section 4.

2. Flow modeling under transcritical conditions

2.1. Computational methodology

The unstructured explicit solver AVBP is used to integrate the compressible Navier–Stokes equations for a multi-species gas [13]. A third order (in time and space) low dissipation centered scheme [14] provides accurate flow solutions [15,16]. Because of the high density gradients encountered in transcritical systems, artificial viscosity is used to avoid spurious oscillations [17], but its level is kept to a minimum. Characteristic boundary conditions are set with the NSCBC method [13,18], adapted to the real gas thermodynamics. For the reacting case, the dynamically thickened flame model (TFLES) can be used in turbulent flow calculations [19–22]. Laminar flame configurations can also be envisaged with the same scheme or, in the present case, with simplified kinetics (1 step – 4 species reaction for O_2/CH_4) in which the reaction rate is determined by an Arrhenius law.

2.2. Real gas thermodynamics

The Peng–Robinson equation of state (PR EOS) [23] is used to model high pressure thermodynamics:

$$p = \frac{\rho r T}{1 - \rho b_m} - \frac{\rho^2 a_m}{1 + 2\rho b_m - \rho^2 b_m^2} \tag{1}$$

where T is the temperature, p the pressure, ρ the density, $r = R/W$ with R being the gas constant and W the molar mass, $a_m(T)$ and b_m are the Peng–Robinson coefficients, which depend on the critical values of the substances involved in the mixture. The latter coefficients are computed using the classical Van Der Waals mixing rules. Details may be found in Poling et al. [24]. Comparisons with the NIST database for pure substances show an excellent agreement in the critical zone and for temperatures higher than the critical temperature. The level of error on the density is small except in the highest density region where it can reach about 10%. This is however considered to be acceptable in view of the important modifications required by a change in the equation of state with consequences on the thermodynamic behavior, and coefficients linked to the equation of state [25]. Complete formulations for the computation of the main thermodynamic functions may be found in [12]. Note that, for consistency, modified thermodynamics have an impact on the formulation of boundary conditions and Jacobian matrices of the numerical schemes.

2.3. Transport models

Pressure gradient contributions to the heat flux and temperature gradient effects on mass transfer may become significant under high pressure conditions. It is, however, possible to neglect the corresponding Dufour and Soret terms because: (1) The scope of the AVBP flow-solver is primarily to perform LES simulations in which the subgrid scale (SGS) fluxes dominate the laminar fluxes; and (2) It has been shown by Oefelein [26] in highly refined simulations that the crossterms in heat and mass fluxes induce weak contributions. The heat flux is then calculated using the classical Fourier expression while mass diffusion is determined using the Hirschfelder–Curtiss approximation [27].

Transport coefficients also feature important real gas effects. The method proposed by Chung et al. [28] is used to determine the viscosity and thermal conductivity. Choosing the same method for these two coefficients yields a significant gain in computational time. The model is based on a low pressure, perfect gas formulation, corrected with an empirical expression to account for high density effects. Used in conjunction with the Peng–Robinson equation of state (PR EOS) [23], the model gives results which closely follow the NIST database. Details on the formulation can be found in [24,28] or [12]. The determination of mass diffusion coefficients in transcritical fluids is less easy because current methods cannot be validated due to a lack of data. This issue is discussed in [12]. It is then reasonable to use constant, species dependent Schmidt numbers to estimate these coefficients from the fluid viscosity. The transcritical version of AVBP includes many additional submodels for the subgrid scale fluxes which are bypassed in the following laminar flow calculations.

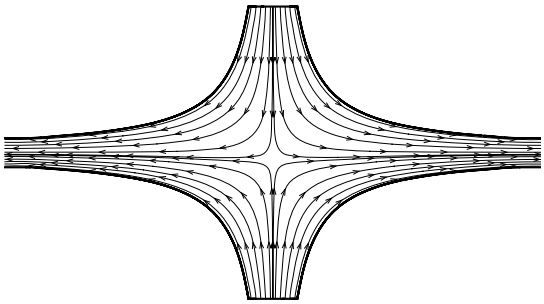

Fig. 1. Typical computational domain and associated stream lines.

3. Methodology for the calculation of multidimensional strained flames

3.1. Methodology

One difficulty in the simulation of counterflow configurations lies in the definition of boundary conditions. If the computational domain is defined as a rectangular box with reactants injected on the two opposite sides of the domain, the lateral conditions are difficult to impose because the jets have free boundaries and their position is not known at the outset. The stagnation plane cannot be stabilized in this situation and oscillates between two locations. One originality of the method adopted in the present study is that the computational domain is bounded by slip walls which fit the streamlines of an ideal counterflow. This geometry serves to guide the flow and obtain a stable stagnation plane. To determine theoretical streamlines, one considers two fluid streams injected from infinity. The flow is assumed to be incompressible and inviscid. Without chemical reaction, the flow is potential and the velocity field is expressed analytically:

$$u = \epsilon_s x, \quad v = -\epsilon_s y \tag{2}$$

where u and v are respectively the transverse and axial components of the velocity vector, x and y are respectively the transverse and axial coordinates, and ϵ_s is the strain rate.

Streamlines determined from Eq. (2) take a hyperbolic shape $xy = \text{cte}$. When considering a reactive flow, this formulation is not entirely valid because the volumetric expansion due to the flame modifies the transverse velocity distribution and changes the streamline pattern. However, for a given pressure and a given strain rate, one can estimate the flame thickness and thus determine the region of influence of the flame in the flow, and specifically on the velocity field. It is then possible to consider a computational domain which is sufficiently large so that the guiding streamlines can be assimilated to those of a potential flow. A typical computational domain is shown in Fig. 1. Streamlines are displayed in the case of a supercritical flow of oxygen impinging on a supercritical methane stream.

The computational domain is meshed with fine cells in the flame and in the density gradient regions, while coarser cells are used elsewhere. The corresponding mesh comprises 80 000 triangular cells and 40 000 nodes. It is terminated by a constant width channel serving to exhaust the burnt stream (Fig. 1). The mesh in this channel becomes coarser as the x coordinate increases so that the flow is diffused before it reaches the outlet. Inlets are treated with characteristic boundary conditions which can be used to impose velocity components, static temperature and mass fraction at the inlet in a numerically "soft" way. The ingoing waves are taken proportional to the difference between the actual state at the boundary nodes and the reference velocity and temperature. Outlets are also treated with characteristic boundary conditions to impose a static pressure. In this formulation the ingoing wave is taken to be proportional to the difference between the actual state at the boundary nodes and the reference value. Other boundaries treated like slip walls behave like streamlines and have only a limited influence on the internal flow.

3.2. Validation of the methodology on multidimensional gaseous strained flames calculations

The previous methodology is validated in the standard case of an oxygen/methane atmospheric strained flames. The oxygen stream, injected at 300 K, impinges on a methane jet, also injected at 300 K, in a 0.1 MPa environment. Injection velocities are variable but correlated in order to keep the same momentum in each injector inlet. The range

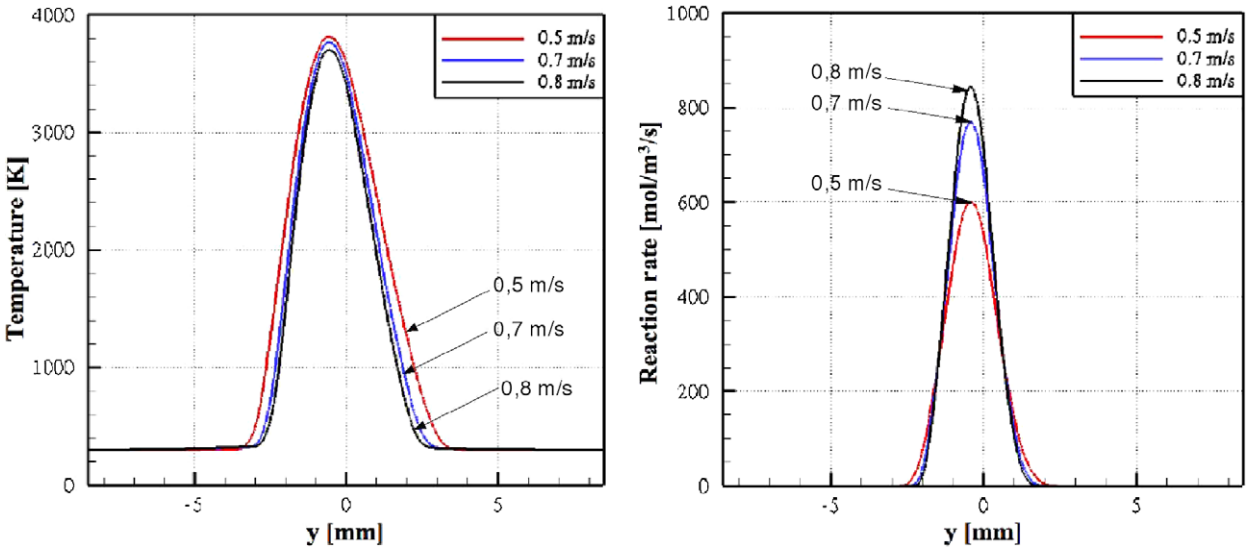

(a) Temperature (b) Reaction rate

Fig. 2. (a) Temperature profiles on the axis, (b) reaction rate profiles on the axis for an atmospheric strained flame formed by oxygen and methane injected at 300 K for several injection velocities.

of velocities considered in this study evolves from 0.5 to 1 $\mathrm{m\,s^{-1}}$. Calculations presented in this section are carried out with the standard AVBP flow solver. The computational domain is based on the geometry of a two-dimensional counterflow burner developed at EM2C.

This simulation of multidimensional strained flames exploits the method described previously to guide the opposed flows by defining a computational domain bounded by the streamlines of an ideal two-dimensional constant strain rate flow. When the injection velocity is low, the flame thickness can be too large to fit into the computational domain, so that the flame is compelled to "retract" to fit in the exhaust channel. However, near the burner axis, the flame is not influenced by the boundary geometry, so that comparisons with self-similar solutions can be carried out. This is treated in the next lines. However, in order to represent the flow dynamics, it is essential to have an a priori estimation of the flame thickness. This key parameter can then be used to build a computational domain which will neither influence nor constrain the flame, but guide the reaction layer and avoid oscillations of the stagnation plane (see Section 3.1).

Fig. 2 displays temperature and reaction rate profiles on the axis of the system for an atmospheric strained flame formed by oxygen and methane injected at 300 K, for several injection velocities. It is well known that the temperature and heat release rate responds to strain rate, and therefore to injection velocity, have an S shape with turning points corresponding to extinction or ignition conditions [29,30]. In the past, these response curves have been obtained using complex chemistry and pseudo arc-length continuation methods [31]. The aim of the present validation is not to retrieve such curves but to capture the evolution of some of the variables, like the maximum flame temperature, flame thickness, heat release rate and reaction rate distribution. Fig. 2(a) shows the temperature profiles obtained by increasing the injection velocity. The maximum flame temperature decreases which is typically found for strained flames, a feature already described in [30]. The flame thickness decreases which corresponds to what one expects from theory. It is known that the thickness scales like the inverse of the square root of the strain rate (see for example [32]). The heat release rate per unit flame surface is known to increase with the strain rate (with the square root of the strain rate when the operating point is sufficiently far from the extinction limit). Close to extinction, the heat release rate decreases sharply and extinction is reached when the tangent becomes vertical. Fig. 2(b) displays the evolution of the reaction rate profile as a function of the injection velocity. The maximum reaction rate increases with increasing injection velocity and so does the integral over the flame zone which can be related to the heat release rate per unit flame area. The main features of the strained flame response to injection velocity variations are retrieved in these multidimensional calculations validating the present methodology.

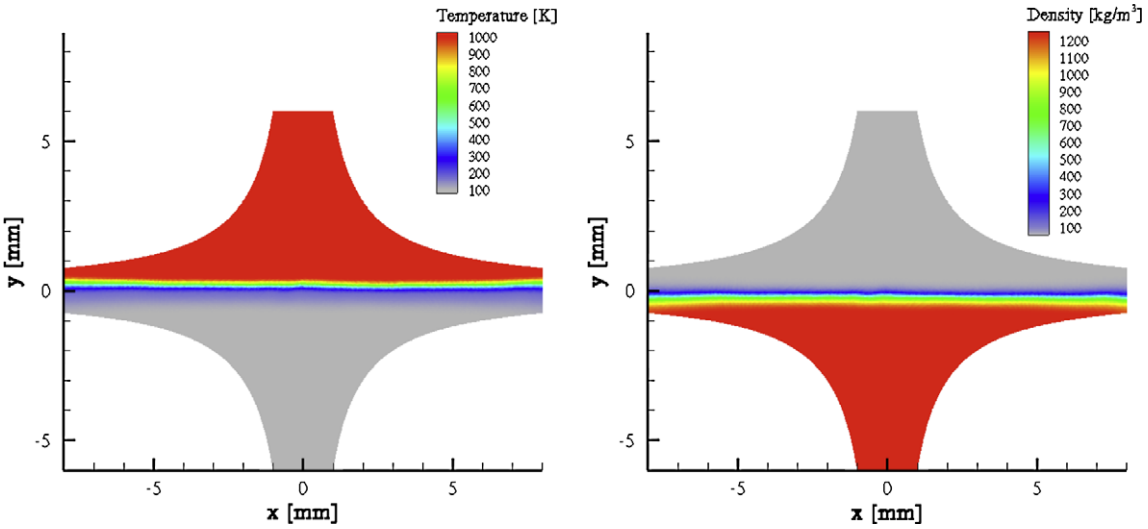

(a) Temperature (b) Density

Fig. 3. Map of density in a non-reacting flow of transcritical oxygen injected at 100 K and 0.5 m s^{-1} impinging on supercritical oxygen (1000 K and 3.4 m s^{-1}) in a 7 MPa environment.

4. Two-dimensional reacting or non-reacting counterflow at high pressure

Three problems are considered successively: (1) A non-reacting opposed flow formed by injecting a transcritical stream of oxygen against a supercritical stream of the same species; (2) A non-premixed strained laminar flame of transcritical oxygen flowing against supercritical methane; (3) A non-premixed flame formed by a stream of transcritical oxygen impinging on a transcritical methane flow. These three situations have been considered in a one-dimensional formulation of the counterflow geometry [12]. The same problems are now envisaged in the multidimensional configuration, to validate the transcritical version of AVBP.

4.1. Counterflow of transcritical and supercritical oxygen

This first case serves to model the more complicated injection process found in high performance liquid-rocket engines where one of the reactants is introduced at a temperature below critical while the ambient pressure is above the critical value, and the environment is at high temperature. The transcritical dense jet of oxygen is surrounded by higher temperature oxygen of much lower density. When heated, this fluid passes continuously from a dense, low-temperature state, to a lighter, high-temperature condition. This transition is effected without crossing an interface between dense and light phases but a region is formed where the mass density rapidly changes as a function of temperature. This high density gradient layer is easily visualized with backlighting [3]. The first configuration considered in this subsection features a structure which includes subcritical and supercritical forms of the same substance. It can be used to estimate the rate of mass transfer between the dense low temperature fluid and the surrounding "vapor". This study aims at providing the rate at which transfer takes place under transcritical injection of oxygen. This quantity is determined as a function of the major parameters influencing this process like the injection velocities (or the strain rate ϵ_s), injection temperature T_{inj}, ambient temperature T_{amb} and critical temperature T_c. The ambient pressure is fixed at a value of 7 MPa which is approximately that used in experiments carried out by Singla et al. [2]. The same calculations repeated at higher pressures yield similar results. Transcritical oxygen is injected at $T_{inj} < T_c$ while the impinging supercritical oxygen jet is injected at 1000 K.

Fields of temperature and density displayed in Fig. 3 correspond to this non-reacting flow of oxygen, where transcritical oxygen is injected at $T_{inj} = 100$ K. The mesh suitably resolves the density gradient layer which is established around $y \simeq -1.5$ mm (Fig. 3(b)). There are about 10 cells in the gradient layer. Transition from the transcritical to the supercritical state, is marked by a large variation in density while the temperature change in this layer is comparatively small (Fig. 3).

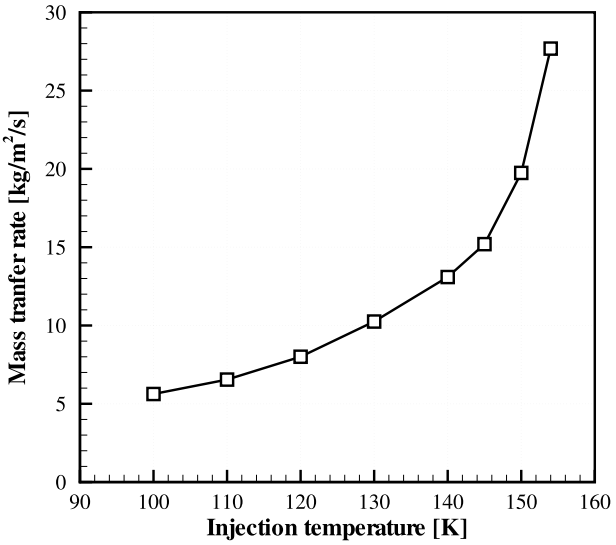

Fig. 4. Evolution of the mass transfer rate with the injection temperature of the transcritical oxygen for a 0.5 m s^{-1} injection velocity. The ambient pressure is fixed at 7 MPa.

As proposed in [11,12], the influence of the injection temperature of the transcritical flow on the mass transfer rate can be cast as a function of a "Spalding-like" number, B_T, defined by:

$$B_T = \frac{T_{amb} - T_c}{T_c - T_{inj}} \tag{3}$$

Fig. 4 shows the evolution of the mass transfer rate as a function of T_{inj} for a given injection velocity. The mass transfer rate increases with the injection temperature of the cold flow. The critical temperature is a singular point in the mass transfer rate expression and this quantity increases as the injection temperature tends to the critical value. This is linked to the definition of this rate and also reflects the physics of the process. The transfer rate is defined as the mass of reactant per unit area and per unit time crossing the critical temperature isosurface. When the injection temperature is close to the critical value less heat is needed to bring the oxygen temperature to the critical value and the mass transferred increases. When injected at the critical value, the oxygen immediately crosses the critical isosurface and the mass transfer rate equals the oxygen mass flow rate injected in the domain. The "Spalding-like" expression given in Eq. (3) reflects the critical temperature singularity found in the multidimensional computations of the mass transfer rate. The mass transfer rate is also found to increase with the strain rate but results are not shown in this article.

4.2. Transcritical strained flames

In this second case, the reactive flow features a transcritical injection of at least one reactant. The structure of a flame produced in a counterflow by a stream of transcritical oxygen impinging on a stream of supercritical methane is considered first. Oxygen injected at $y = -30$ mm at 1 m s^{-1} is in a transcritical state ($T_{\mathrm{LOx}} = 80$ K), with a liquid-like density of $\rho_{\mathrm{LOx}} = 1300$ kg m^{-3} whereas methane, injected at $y = 30$ mm at 300 K, has a density close to that of a perfect gas at a pressure of 7 MPa $\rho_{\mathrm{CH_4}} = 50$ kg m^{-3}. Figs. 5(a) to 5(d) display typical distributions of temperature, density, oxygen mass fraction and heat release rate for these conditions. The flame is nearly flat and its thickness is about 1 mm. This value is slightly overestimated by comparison with our previous study of transcritical counterflow flames in a one-dimensional formulation [12]. This deviation is most probably related to the different models used in the present flow solver. The flame temperature (Fig. 5(a)) is about 3850 K which is close to the expected maximum temperature at this pressure. The flame features a sharp density gradient on the oxygen side (Fig. 5(b)), which is typical of transcritical injection. The existence of such a layer is well observed in transcritical flame experiments [2] or in the transcritical injection of non-reactive jets [33] and it is here well obtained numerically. Transcritical injection also features a drop in oxygen diffusion (Fig. 5(c)). The oxygen mass fraction evolves more abruptly than that of methane,

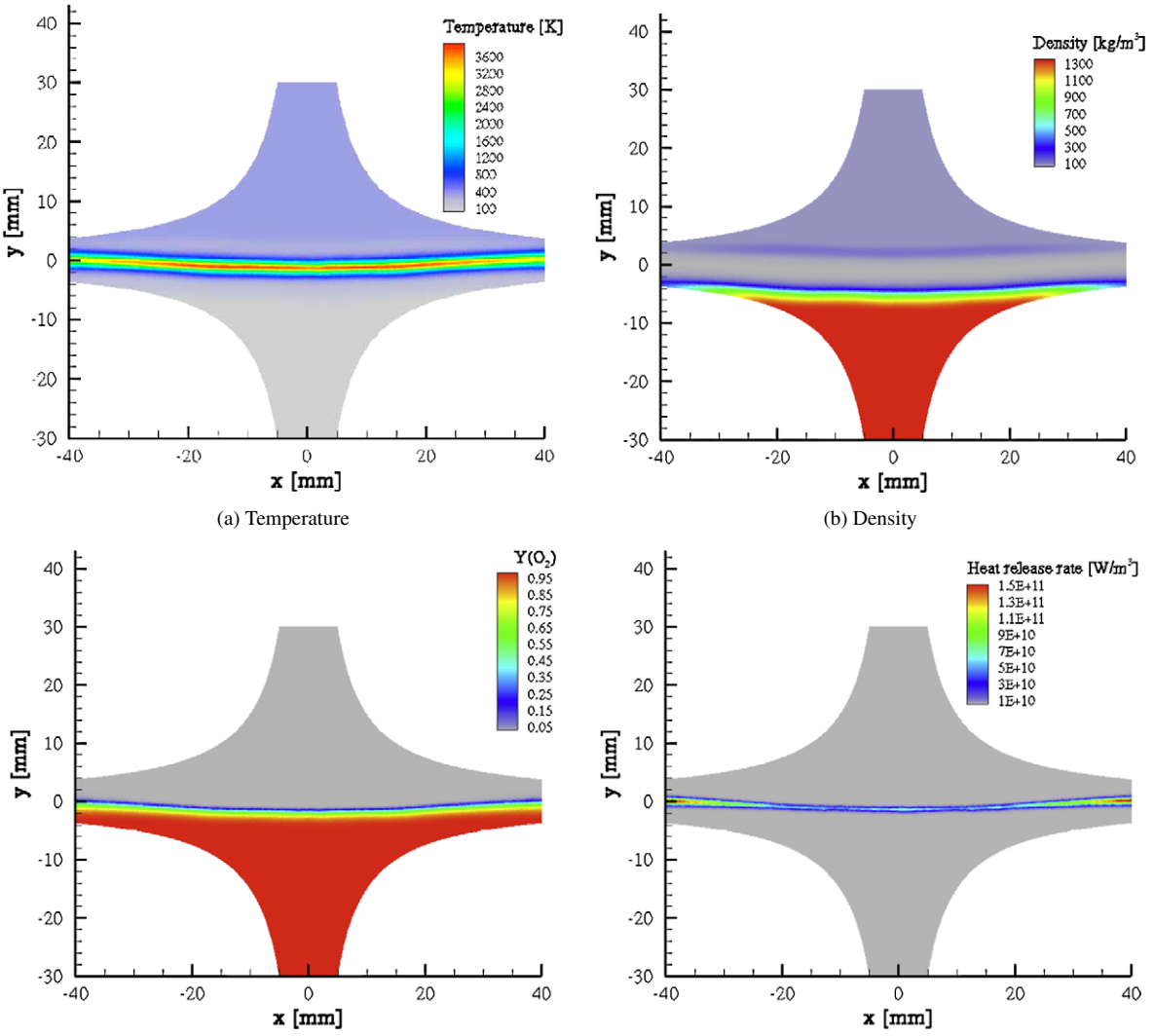

(a) Temperature

(b) Density

(c) Oxygen mass fraction

(d) Heat release rate

Fig. 5. Maps of temperature (a), density (b), oxygen mass fraction (c) and heat release rate (d) of a strained flame formed by a transcritical stream of oxygen injected at 80 K and 1 m s^{-1} impinging on a supercritical methane stream at 300 K and 5 m s^{-1} in a 7 MPa environment.

injected in a supercritical state. Because of the single-step chemistry used in the present study, it is not possible to compare local heat release rate values with results obtained with complex kinetics and multispecies transport [12]. However, the order of magnitude of the maximum heat release rate is retrieved. The flame is established in the low density region and the dense oxygen acts like a nearly impermeable boundary to the flame as already remarked in [12].

In the third case which is not often considered, both reactants are injected under transcritical conditions. The chamber pressure of 7 MPa exceeds the critical values for oxygen ($p_c(O_2) = 5.04$ MPa) and methane ($p_c(CH_4) = 4.59$ MPa), and the methane temperature is reduced to 110 K a value which is below its critical temperature $T_c(CH_4) = 190.564$ K. The reactant densities of methane $\rho_{LCH_4} = 485$ kg m^{-3} and oxygen $\rho_{LOx} = 1350$ kg m^{-3} have similar orders of magnitude. Because methane and oxygen are injected in similar thermodynamical states, the temperature profile is more symmetric than in the previous case. The flame now features two strong density gradients on its two sides (Fig. 6) and chemical conversion is confined in the low density region. By comparing temperature and density profiles it can be seen that the flame develops in the intermediate region separating the two transcritical streams and occupied by light gases. The dense streams on the two sides of the flame constitute nearly impermeable boundaries constraining the reactive layer. However, it is found that a small amount of reaction products is transported in the

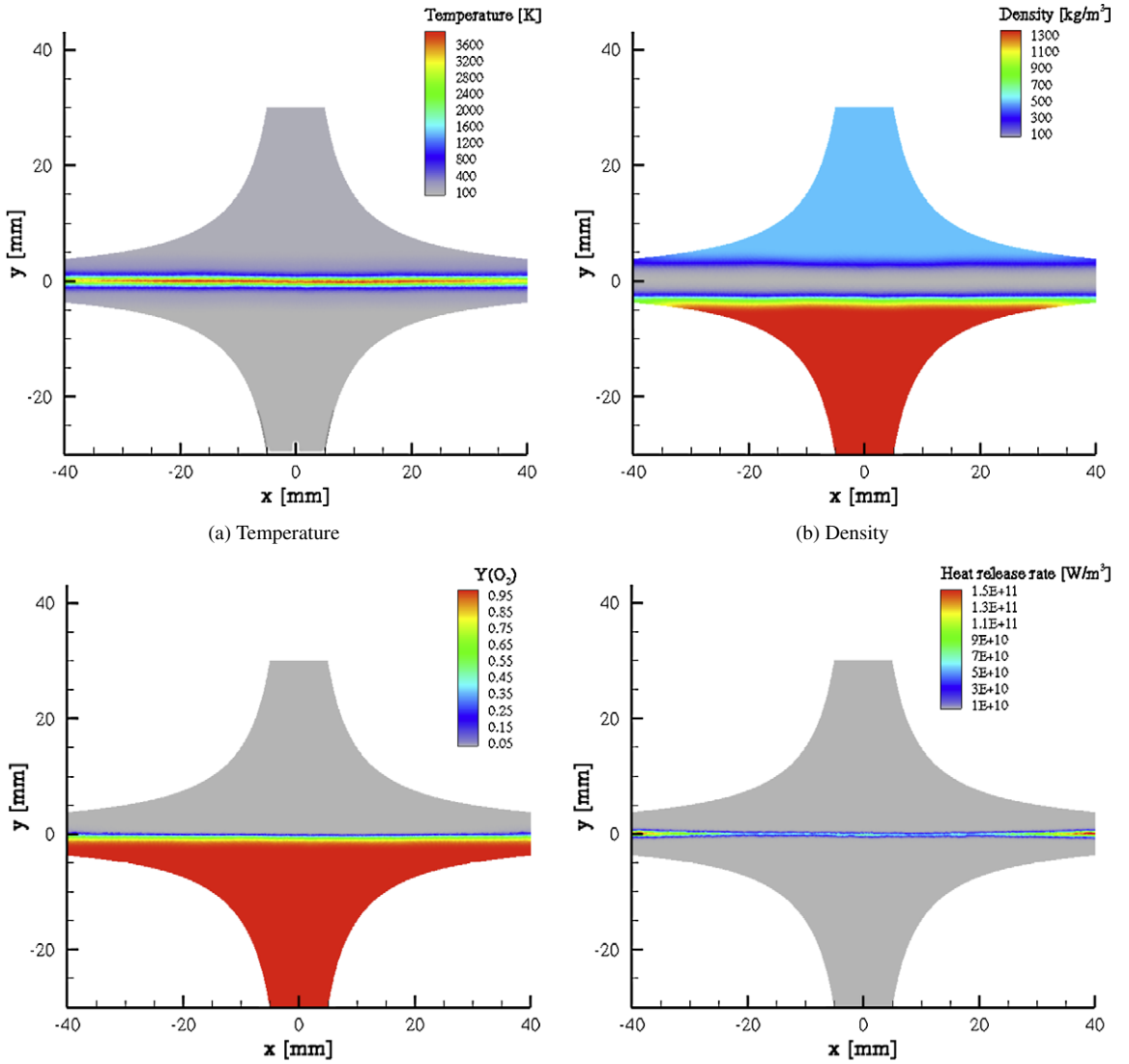

(a) Temperature

(b) Density

(c) Oxygen mass fraction

(d) Heat release rate

Fig. 6. Maps of temperature (a), density (b), oxygen mass fraction (c) and heat release rate (d) of a strained flame formed by a transcritical stream of oxygen injected at 80 K and 1 m s^{-1} impinging on a supercritical methane stream at 110 K and 1.6 m s^{-1} in a 7 MPa environment.

low temperature regions, due to their high diffusivity in the supercritical regime. Transcritical oxygen and methane are heated by the flame before they react in the non-premixed flame yielding very sharp density gradient layers. The consequence is that the rate of burning is controlled by mass transfer from the dense reactants justifying the study carried out on the transfer rate of mass from the dense transcritical region to the lighter surroundings.

5. Conclusions

This article proposes a method for simulating transcritical combustion in multidimensional strained flame configurations and illustrates this treatment with sample calculations. Real gas effects and transport anomalies are included in the flow solver (AVBP) which can be used to simulate high pressure, low temperature transcritical flows. The numerical technique is modified to resolve in a suitable manner density gradients inherent to transcritical injection. The transcritical version of AVBP is used to study generic problems involving reactants injected in a transcritical state. The configuration chosen in this study is that of a counterflow which is often used to model the local structure of turbulent

flames. The counterflow of a stream of transcritical oxygen impinging on a supercritical stream of the same species is considered first. This problem is used to simulate the behavior of a dense pocket surrounded by its own vapor. The structure of this flow is calculated numerically and the mass transfer rate from the dense region is determined as a function of strain rate and injection temperature of the transcritical stream. A recent correlation which involves a "Spalding-like" transfer number and the square root of the strain rate is confirmed by the present multidimensional simulations. Supercritical methane/transcritical oxygen flames are treated as a second example. The pressure is above critical but the oxygen temperature is below critical. The flame structure features a strong density gradient on the oxygen side of the flame. The density of oxygen drops by two orders of magnitude between the injected stream and the flame region. Reactive flow simulations are also carried out in the non-standard case where both methane and oxygen are injected in transcritical states. The calculations feature strong density gradients which are established on the two sides of the flame and confine the reactive layer in the light region formed between the two dense streams. The rate of burning is controlled in this case by mass transfer from the transcritical regions.

Acknowledgements

This work has been supported by Snecma the prime contractor for the European launcher Ariane 5 cryogenic propulsion systems, CNES and CNRS.

References

[1] M. Juniper, A. Tripathi, P. Scouflaire, C. Rolon, S. Candel, The structure of cryogenic flames at elevated pressures, Proceedings of the Combustion Institute 28 (2000) 1103–1110.
[2] G. Singla, P. Scouflaire, C. Rolon, S. Candel, Transcritical oxygen/transcritical or supercritical methane combustion, Proceedings of the Combustion Institute 30 (2005) 2921–2928.
[3] M. Oschwald, J.J. Smith, R. Branam, J. Hussong, A. Schick, Injection of fluids into supercritical environments, Combustion Science and Technology 178 (1–3) (2006) 49–100.
[4] K.G. Harstad, R.S. Miller, J. Bellan, Efficient high-pressure state equations, AIChE Journal 43 (1997) 1605–1610.
[5] R.S. Miller, K.G. Harstad, J. Bellan, Direct numerical simulations of supercritical fluid mixing layers applied to heptane–nitrogen, Journal of Fluid Mechanics 436 (2001) 1–39.
[6] N. Okong'o, K. Harstad, J. Bellan, Direct numerical simulations of O_2/H_2 temporal mixing layers under supercritical conditions, AIAA Journal 40 (5) (2002) 914–926.
[7] L. Selle, N. Okong'o, J. Bellan, K.G. Harstad, Modelling of subgrid-scale phenomena in supercritical transitional mixing layers: an a priori study, Journal of Fluid Mechanics 593 (2007) 57–91.
[8] N. Zong, V. Yang, Near-field flow and flame dynamics of LOX/methane shear-coaxial injector under supercritical conditions, Proceedings of the Combustion Institute 31 (2) (2007) 2309–2317.
[9] W.A. Sirignano, J.-P. Delplanque, Transcritical vaporization of liquid fuels and propellants, Journal of Propulsion and Power 15 (6) (1999) 896–902.
[10] K.G. Harstad, J. Bellan, An all-pressure fluid drop model applied to a binary mixture: heptane in nitrogen, International Journal of Multiphase Flow 26 (10) (2000) 1675–1706.
[11] V. Yang, Modeling of supercritical vaporization, mixing, and combustion processes in liquid-fueled propulsion systems, Proceedings of the Combustion Institute 28 (2000) 925–942.
[12] L. Pons, N. Darabiha, S. Candel, G. Ribert, V. Yang, Mass transfer and combustion in transcritical non-premixed counterflows, Combustion Theory and Modelling 13 (2009) 57–81.
[13] V. Moureau, G. Lartigue, Y. Sommerer, C. Angelberger, O. Colin, T. Poinsot, Numerical methods for unsteady compressible multi-component reacting flows on fixed and moving grids, Journal of Computational Physics 202 (2) (2005) 710–736.
[14] O. Colin, F. Ducros, D. Veynante, T. Poinsot, A thickened flame model for large eddy simulations of turbulent premixed combustion, Physics of Fluids 12 (7) (2000) 1843–1863.
[15] A.G. Kravchenko, P. Moin, R. Moser, Zonal embedded grids for numerical simulations of wall-bounded turbulent flows, Journal of Computational Physics 127 (2) (1996) 412–423.
[16] J. Gullbrand, F.K. Chow, The effect of numerical errors of turbulence models in large eddy simulations of channel flow, with and without explicit filtering, Journal of Fluid Mechanics 495 (2003) 323–341.
[17] A. Jameson, W. Schmidt, E. Turkel, Numerical solution of the Euler equations by finite volume methods using Runge–Kutta time stepping schemes, in: 14th Fluid and Plasma Dynamic Conference, AIAA Paper 1981-1259, 1981.
[18] T. Poinsot, T. Echekki, M.G. Mungal, A study of the laminar flame tip and implications for premixed turbulent combustion, Combustion Science and Technology 81 (1–3) (1992) 45–73.
[19] P. Schmitt, T.J. Poinsot, B. Schuermans, K. Geigle, Large-eddy simulation experimental study of heat transfer, nitric oxide emissions and combustion instability in a swirled turbulent high pressure burner, Journal of Fluid Mechanics 570 (2007) 17–46.
[20] J.P. Légier, T. Poinsot, D. Veynante, Dynamically thickened flame LES model for premixed and non-premixed turbulent combustion, in: Proceedings of the Summer Program, Center for Turbulence Research, NASA Ames/Stanford Univ., 2000, pp. 157–168.

[21] C. Martin, L. Benoit, Y. Sommerer, F. Nicoud, T. Poinsot, LES and acoustic analysis of combustion instability in a staged turbulent swirled combustor, AIAA Journal 44 (4) (2006) 741–750.
[22] A. Sengissen, A. Giauque, G. Staffelbach, M. Porta, W. Krebs, P. Kaufmann, T. Poinsot, Large eddy simulation of piloting effects on turbulent swirling flames, Proceedings of the Combustion Institute 31 (2007) 1729–1736.
[23] D. Peng, D.B. Robinson, A new two-constant equation of state, Industrial and Engineering Chemistry Fundamentals 15 (1976) 59–64.
[24] B.E. Poling, J.M. Prausnitz, J.P. O'Connel, The Properties of Gases and Liquids, fifth edition, McGraw–Hill, 2001.
[25] R. Dehoff, Thermodynamics in Materials Science, second edition, Taylor & Francis, 2006.
[26] J.C. Oefelein, Large eddy simulation of a shear-coaxial LOX-H_2 jet at supercritical pressure, in: 38th AIAA/ASME/SAE/ASEE Joint Propulsion Conference and Exhibit, AIAA Paper 2002-4030, 2002.
[27] J.O. Hirschfelder, C.F. Curtiss, R.B. Bird, Molecular Theory of Gases and Liquids, John Wiley & Sons, 1954.
[28] T.H. Chung, M. Ajlan, L.L. Lee, K.E. Starling, Generalized multiparameter correlation for nonpolar and polar fluid transport properties, Industrial and Engineering Chemistry Research 27 (4) (1988) 671–679.
[29] N. Darabiha, S.M. Candel, V. Giovangigli, M.D. Smooke, Extinction of strained premixed propane–air flames with complex chemistry, Combustion Science and Technology 60 (4–6) (1988) 267–285.
[30] A. Liñan, Asymptotic structure of counterflow diffusion flames for large activation-energies, Acta Astronautica 1 (7–8) (1974) 1007–1039.
[31] N. Darabiha, S. Candel, The influence of the temperature on extinction and ignition limits of strained hydrogen–air diffusion flames, Combustion Science and Technology 27 (1992) 269–285.
[32] L. Pons, N. Darabiha, S. Candel, Pressure effects on non-premixed strained flames, Combustion and Flame 152 (1–2) (2008) 218–229.
[33] B. Chehroudi, D. Talley, E. Coy, Initial growth rate and visual characteristics of a round jet into a sub- to supercritical environment of relevance to rocket, gas turbine and diesel engines, in: AIAA 37th Aerospace Science Meeting and Exhibit, AIAA Paper 1999-16128, 1999.